Original Article

MOLECULAR METABOLISM

Endothelial arginase 2 mediates retinal ischemia/reperfusion injury by inducing mitochondrial dysfunction

Esraa Shosha [1,2,3,4], Abdelrahman Y. Fouda [1,2,3,4], Tahira Lemtalsi [1,3,4], Stephen Haigh [1], David Fulton [1], Ahmed Ibrahim [3,5,6], Mohamed Al-Shabrawey [3,7], R. William Caldwell [3,8], Ruth B. Caldwell [1,3,4,*]

ABSTRACT

Objective: Retinal ischemic disease is a major cause of vision loss. Current treatment options are limited to late-stage diseases, and the molecular mechanisms of the initial insult are not fully understood. We have previously shown that the deletion of the mitochondrial arginase isoform, arginase 2 (A2), limits neurovascular injury in models of ischemic retinopathy. Here, we investigated the involvement of A2-mediated alterations in mitochondrial dynamics and function in the pathology.

Methods: We used wild-type (WT), global A2 knockout (A2KO-) mice, cell-specific A2 knockout mice subjected to retinal ischemia/reperfusion (I/R), and bovine retinal endothelial cells (BRECs) subjected to an oxygen-glucose deprivation/reperfusion (OGD/R) insult. We used western blotting to measure levels of cell stress and death markers and the mitochondrial fragmentation protein, dynamin related protein 1 (Drp1). We also used live cell mitochondrial labeling and Seahorse XF analysis to evaluate mitochondrial fragmentation and function, respectively.

Results: We found that the global deletion of A2 limited the I/R-induced disruption of retinal layers, fundus abnormalities, and albumin extravasation. The specific deletion of A2 in endothelial cells was protective against I/R-induced neurodegeneration. The OGD/R insult in BRECs increased A2 expression and induced cell stress and cell death, along with decreased mitochondrial respiration, increased Drp1 expression, and mitochondrial fragmentation. The overexpression of A2 in BREC also decreased mitochondrial respiration, promoted increases in the expression of Drp1, mitochondrial fragmentation, and cell stress and resulted in decreased cell survival. In contrast, the overexpression of the cytosolic isoform, arginase 1 (A1), did not affect these parameters.

Conclusions: This study is the first to show that A2 in endothelial cells mediates retinal ischemic injury through a mechanism involving alterations in mitochondrial dynamics and function.

Keywords Retina; Ischemia; Arginase; Endothelial cells; Mitochondria

1. INTRODUCTION

Retinal ischemia is a prominent feature in blinding eye diseases like central vein occlusion, acute glaucoma, and retinopathy of prematurity. Available treatments target late-stage pathology, underscoring the critical need for developing new therapies to limit the initial insult. Retinal ischemia is characterized by sequential events of calcium overload, oxidative stress, inflammation, and neurovascular degeneration [1,2]. Retinal ischemia/reperfusion (I/R) models have been widely used to study the molecular mechanism involved in retinal ischemic disease [3–5]. We have previously shown that the reactive oxygen species (ROS) generating the enzyme NOX2 NADPH oxidase plays a role in promoting neurodegeneration after the retinal I/R insult [4]. NOX2 deletion significantly protected against I/R-induced neuronal cell death and glial activation through a mechanism involving decreased oxidative stress and reduced activation of cell stress pathways [4]. In a subsequent study, we found that a downstream target of NOX2, the arginase 2 ureahydrolase enzyme, is involved in I/R-induced neurovascular injury [3].

Arginase hydrolyzes the amino acid L-arginine to form ornithine and urea. It plays a vital role in ammonia detoxification through the urea cycle and in cell proliferation through the formation of L-ornithine, a precursor for polyamines and L-proline [6]. It exists in 2 isoforms, the cytosolic isoform arginase 1 (A1) and the mitochondrial isoform arginase 2 (A2) [7]. Both isoforms are expressed in various organs, including the liver, kidney, brain, prostate [8], and retina [9–11]. Arginase activity has been implicated in the I/R insult in different organs, including the heart, kidney, and liver [12–14]. In a previous

[1]Vascular Biology Center, Augusta University, Augusta, GA, USA [2]Department of Clinical Pharmacy, Faculty of Pharmacy, Cairo University, Cairo, Egypt [3]Vision Discovery Institute, Augusta University, Augusta, GA, USA [4]Charlie Norwood VA Medical Center, Augusta, GA, USA [5]Wayne State University, Department of Ophthalmology, Visual, and Anatomical Sciences, Department of Pharmacology, Detroit, MI, USA [6]Department of Biochemistry, Faculty of Pharmacy, Mansoura University, Mansoura, Egypt [7]Department of Oral Biology, Dental College of Georgia, Augusta, GA, USA [8]Department of Pharmacology and Toxicology, Augusta University, Augusta, GA, USA

*Corresponding author. Medical College of Georgia, Augusta University, 1460 Laney Walker Blvd, CB 3209A, Augusta, GA 30912, USA. E-mail: rcaldwel@augusta.edu (R.B. Caldwell).

Received April 15, 2021 • Revision received June 5, 2021 • Accepted June 11, 2021 • Available online 15 June 2021

https://doi.org/10.1016/j.molmet.2021.101273

study, we found that A2 expression significantly increased after the retinal I/R insult [3]. A2 deletion significantly protected against I/R-induced neurodegeneration, prevented capillary degeneration, and preserved inner retinal function. The data indicated that A2 promotes neurovascular degeneration through a mechanism involving the increased formation of superoxide and peroxynitrite and activation of the mitogen activated protein kinase (MAPK) stress pathway [3]. We have shown that A2 expression is also involved in neurodegeneration and pathological neovascularization in a mouse model of oxygen-induced retinopathy [10,11,15]. The damage was attributed to increased oxidative stress, NOS uncoupling, and the activation of polyamine pathways. The A2 enzyme is implicated in other central nervous system injuries as well, such as Alzheimer's disease and traumatic brain injuries [16,17]. In contrast with the damaging effects of A2, we have also shown that the cytosolic A1 isoform has protective effects through promoting macrophage-mediated repair in the mouse model of retinal I/R injury [18].

Thus, previous studies have provided evidence for the involvement of A2 in promoting vascular injury in the ischemic retina. However, the exact mechanisms remain unclear. Given the mitochondrial localization of A2, we investigated its potential role in inducing vascular injury via its effects on mitochondrial function and dynamics.

2. RESULTS

2.1. A2 deletion limits I/R-induced retinal detachment/edema and reduces breakdown of the blood-retinal barrier

Previous histological studies from our group and other researchers have shown disruption of the retinal structure and the breakdown of the blood-retinal barrier after an I/R insult [3,4,19]. Here, we used fundus imaging and optical coherence tomography (OCT) to examine the impact of A2 deletion on the I/R-induced retinal damage in living mice. Fundus imaging and OCT are non-invasive approaches used in humans and animals to assess retinal structural abnormalities. Fundus imaging of wild-type (WT) retinas at 7 days after I/R injury showed a distorted fundus with numerous areas of apparent swelling (arrows), whereas the retinas of the A2KO mice appeared similar to the sham controls (Figure 1A). OCT optical scanning of WT retinas showed significant disruption of the retinal structure with areas of retinal detachment and apparent edema (arrows, Fig. 1B), suggesting the disruption of the outer blood-retinal barrier. A2 knockout (A2KO) mice had a less distorted fundus and more preserved retinal structure than WT mice and displayed no evidence of detachment or edema. We re-evaluated the same mice 5 weeks after the injury and found that the detachment and apparent edema were resolved (Fig. S1).

We investigated the effect of the A2 deletion on I/R-induced increases in retinal vascular permeability to confirm the protective effects of the A2 deletion in limiting the I/R-induced retinal edema and detachment. We measured albumin extravasation in perfused retinas by western blot, as previously described [18]. This analysis showed that the albumin extravasation after I/R deletion was significantly reduced in the A2 retinas compared to the WT mice (Figure 2A&B). These results suggest that A2 expression is not only crucial for retinal vascular injury but also has a role in the damage to the RPE and outer blood-retinal barrier.

2.2. Endothelial cell-specific deletion of A2 protects against I/R-induced neurodegeneration

We have previously shown that the global deletion of A2 limits the formation of acellular capillaries and prevents I/R-induced neurodegeneration, whereas the hemizygous deletion of A1 worsens both pathologies [3]. Moreover, the neuroprotective effects of A1 were found to be myeloid cell-specific [18]. The protective effects of the A2 deletion in limiting capillary degeneration and preserving blood-retinal barrier function suggest that the A2 expression within the vascular endothelial cells could be a key mediator of I/R injury. We investigated this possibility by determining and comparing the effects of endothelial cell- or myeloid cell-specific deletion of A2 (E-A2KO or M-A2KO, respectively) on neuronal cell loss after I/R injury. Un-injured retinas from E-A2KO, M-A2KO, and LoxP controls showed no histological difference, as examined by H&E staining (Fig. S2). After I/R, retinas from E-A2KO mice showed significant neuroprotection, as indicated by increased numbers of NeuN positive cells compared with retinas from LoxP controls (Figure 3A&B). A2 deletion in myeloid cells did not alter the I/R-induced neuronal loss (Figure 3A&B). This finding indicates that A2 expression within the vascular endothelial cells plays a vital role in ischemic injury.

2.3. OGD/R-induced increases in cell stress, cell death, and mitochondrial dysfunction are associated with increased A2 expression

To better dissect the role of arginase in promoting endothelial cell injury, we set up an in vitro model of oxygen-glucose deprivation (OGD). Bovine retinal endothelial cells (BRECs) were placed in a glucose-free media and exposed to hypoxia (OGD) to simulate the ischemic phase of I/R. The cells were then returned to normoxia, and the media was changed to the normal complete media to simulate the reperfusion phase (R). After 6 h (hr) of OGD, followed by 6 h of R, the expression of A2, but not A1, was increased (Figure 4A—D). The OGD/R-induced increase in A2 expression was accompanied by a significant increase in cell stress, as shown by the increased phosphorylation of p38 MAPK (P-p38 MAPK; Figure 4E,F) and cell death, as indicated by cleavage of poly (ADP-ribose) polymerase (PARP; Figure 4E,G). The increase in P-p38 MAPK was significantly inhibited by treatment with the global arginase inhibitor 2(S)-amino-6-boronohexanoic Acid (ABH), but cell death as measured by cleaved PARP and LDH release assay was not significantly changed (Figure 4E—G, Fig. S3).

Mitochondria are highly dynamic organelles. They undergo fission and fusion in a well-balanced manner, depending on the cell type and context. Alterations in mitochondrial dynamics have been implicated in retinal I/R injury. Several studies have reported that mitochondrial fission is increased after OGD in endothelial cells and neurons [20—22]. Analysis of the expression levels of the fission protein dynamin related protein 1 (Drp1) after 6 h OGD/6 h R showed that Drp1 expression was significantly reduced by arginase inhibition (Figure 5A,B). The mitochondrial content was not changed, as shown by the comparable protein levels of the mitochondrial marker Voltage-dependent anion channel (VDAC; Fig. 5A). We further analyzed the mitochondrial structure using the cationic dye Rhodamine 123 to label the mitochondria in living endothelial cells. In normoxic conditions, the mitochondrial morphology was normal, with tubular, highly-interconnected mitochondria (Fig. 5C). After OGD/R, the mitochondria were fragmented and punctate (Fig. 5C). ABH treatment partially restored the mitochondrial morphology under OGD/R conditions (Fig. 5C).

Additionally, we examined the effect of OGD/R on mitochondrial function using a Seahorse XF96 instrument. We chose a shorter duration of OGD/R for these studies because our preliminary studies and previous publications showed that OGD/R effects on mitochondria begin soon after the return to normoxia [23]. BRECs were subjected to 5 h OGD, followed by 1 h R. Following the OGD/R, mitochondrial function was measured by tracking the oxygen consumption rate

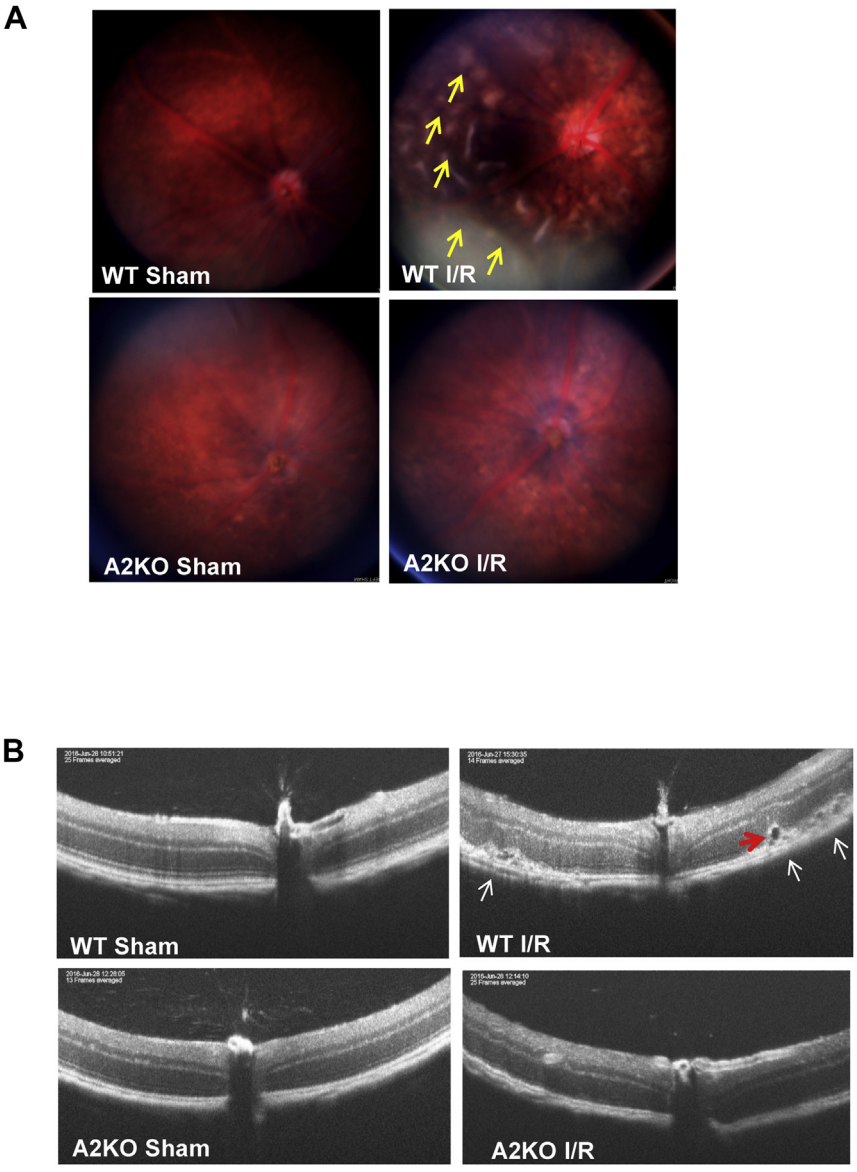

Figure 1: A2 deletion preserves retinal structure and prevents retinal detachment. A) Fundus images showing distorted fundus (arrows) in WT mice 1 week after I/R injury. This alteration was markedly prevented in A2KO mice. n = 4–5. B) Optical coherence tomography (OCT) images showing significant distortion of retinal layers, retinal detachment (white arrows), and edema (red arrow) in WT retinas 1 week after I/R injury. Retinal structure in the A2KO retinas was largely preserved, and retinal detachment was not evident. n = 4–5.

(OCR), following injections of selected compounds provided in the Mitostress kit. The basal respiration rate was measured before injecting any compounds. This measurement showed that basal respiration was decreased after OGD/R compared to normoxia (Fig. 5E). The OCR was further decreased in both groups with oligomycin injection and was increased in normoxic conditions with the injection of the uncoupler FCCP (Fig. 5E). FCCP simulates physiological energy demand conditions. BRECs subjected to normoxic conditions responded to increased energy demand, as shown by a marked increase in the OCR. This effect was markedly blunted in cells subjected to OGD/R. The maximal respiration rate measured after FCCP injection was significantly reduced with OGD/R (Figure 5E&F). Spare respiratory capacity calculated by subtracting the basal respiration from the maximal respiration was also significantly reduced after OGD/R compared to normoxic conditions (Figure 5E&G). The OGD/R insult also significantly reduced the glycolysis parameter, extracellular acidification rate (ECAR; Fig. 5H). The ABH treatment did not alter the OGD/R-induced mitochondrial dysfunction. This effect could be due to ABH's ability to inhibit both A1 and A2, which may have opposing effects.

2.4. Overexpression of A2 in endothelial cells increases mitochondrial fragmentation and impairs mitochondrial respiration

We overexpressed each isoform in BRECs using adenoviral vectors (AAV) to dissect the specific roles of A1 versus A2 in the mitochondrial structure and function in endothelial cells. We used adenoviral vectors expressing red fluorescence protein (RFP) to visualize the transduction efficacy. Fluorescence imaging of RFP confirmed the transduction of the BRECs (Figure 6A). Western blot analysis confirmed the overexpression of A2 and A1 (Figure 6B&C) in BRECs transduced with wild-type A2 (A2), wild-type A1 (A1), or inactive mutant A1 (ΔA1) adenoviral

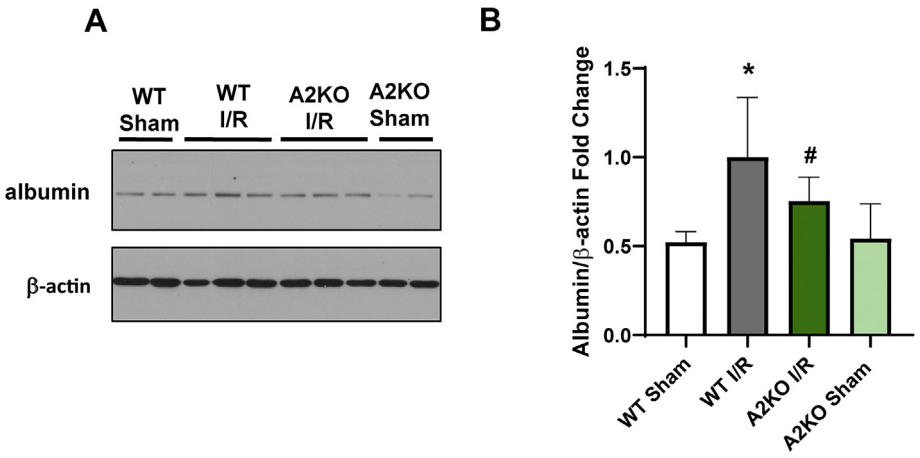

Figure 2: A2 deletion protects against I/R-induced permeability. A) Western blotting analysis with quantification (B) showing a significant decrease in extravascular albumin levels in A2KO retinas after I/R injury compared to WT retinas. *p $<$ 0.05 vs. WT Sham, #p $<$ 0.05 vs. WT I/R. n $=$ 6–7. Data are presented as mean $\pm$ SD.

vectors, respectively, compared to cells transduced with RFP viral vectors.

As mentioned earlier, A1 is primarily localized in the cytosol, and A2 is localized in the mitochondria. We isolated the mitochondrial and cytosolic fractions from BRECs after overexpressing the different AAV constructs to confirm the mitochondrial localization of the overexpressed A2 protein. The overexpressed A2 protein is primarily localized in the mitochondrial fraction compared to the cytosolic fraction (Fig. 6D). Voltage-dependent anion channel (VDAC) and glyceraldehyde 3-phosphate dehydrogenase (GAPDH) were used as mitochondrial and cytosolic markers, respectively.

We determined the effects of A1 and A2 overexpression on mitochondrial fragmentation by western blot analysis of Drp1 expression and live cell imaging of mitochondrial labeling. The overexpression of A2 but not A1 significantly increased Drp1 levels compared with the RFP and ΔA1 controls (Figure 6E–H). Confocal imaging of Rhodamine 123 demonstrated that the overexpression of A2 but not A1 increased mitochondrial fragmentation compared to BRECs overexpressing the green fluorescence protein (GFP) control (Figure 6I&J).

We investigated the effect of overexpression of A1 and A2 on mitochondrial function utilizing Seahorse XF technology. Under normoxic conditions, mitochondrial function was significantly impaired following overexpression of A2, as shown by the significant reductions in basal respiration, maximal respiration, ATP production, and spare respiratory capacity compared to the RFP control (Figure 7A–E). Seahorse XF analysis of mitochondrial function after OGD/R showed a significant

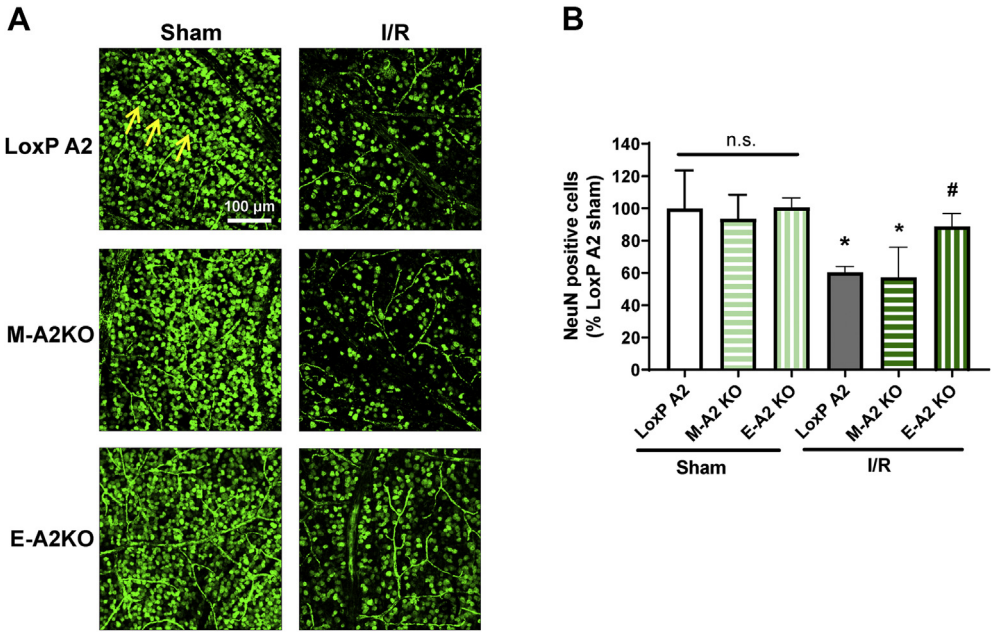

Figure 3: A2 cell-specific deletion in endothelial cells reduced I/R-induced neurodegeneration. A) Confocal imaging of retinal flatmounts labeled with the neuronal marker (NeuN) and quantification (B) showing a significant increase in NeunN positive cells (arrows) in endothelial specific A2 Knockout (E-A2 KO) retinas subjected to I/R. LoxP mice were used as controls. Data are presented as percent of LoxP sham. Myeloid specific A2 knockout (M-A2 KO) did not show protection against I/R-induced neuronal loss. Data are presented as mean $\pm$ SD.

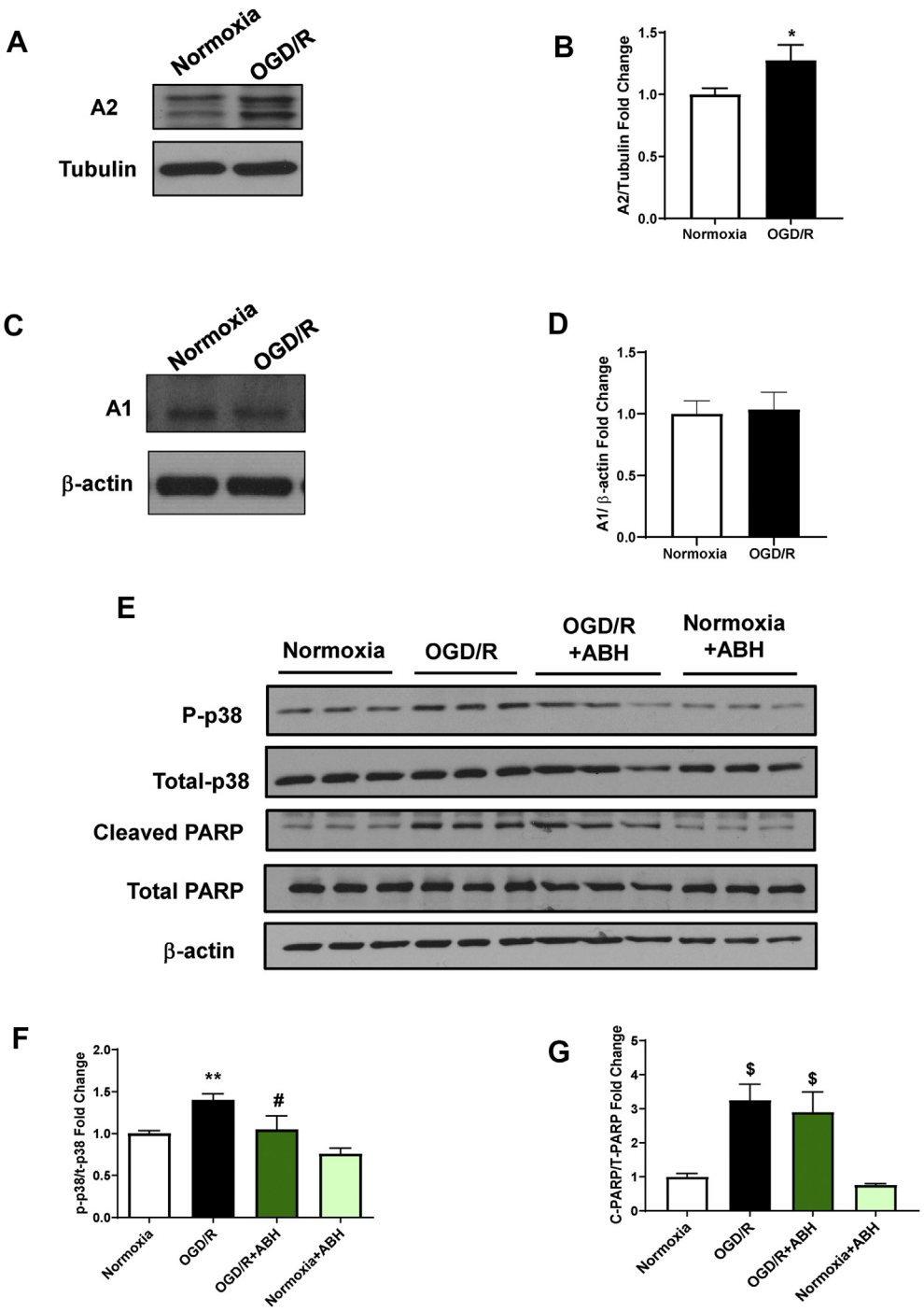

Figure 4: OGD/R induces an increase in A2 expression along with increases in cell stress in BREC, and arginase inhibition prevented this effect. A) and C) Western blot analysis with quantification (B and D) showing increased expression of A2 after OGD/R in BRECs compared to normoxia. There was no change in A1 protein levels. *P $<$ 0.05 vs. normoxia. n $=$ 3. E) Western blot analysis with quantification (F and G) showing increased protein levels of phospho p38MAPK and cleaved PARP after OGD/R in BRECs compared to normoxia. ABH treatment significantly protected against OGD/R-induced phosphorylation of p38. **P $<$ 0.01 vs. Normoxia, #P $<$ 0.01 vs. OGD/R, $p $<$ 0.001 vs. Normoxia. n $=$ 3. Data are presented as mean $\pm$ SD.

decrease in basal respiration and spare respiratory capacity, indicating mitochondrial dysfunction in the OGD/R RFP and OGD/R ΔA1 groups (Fig. 7). However, the OGD/R treatment of BRECs transduced with A2 did not induce any further deterioration in their mitochondrial function, indicating that A2 overexpression and OGD/R insult can induce comparable alterations in mitochondrial function. We further examined mitochondrial fission in vivo by measuring Drp1 levels. I/R injury resulted in more than a 10-fold increase in retinal Drp1 expression, which was decreased with A2 deletion, though this reduction was not statistically significant (Fig. S4).

In contrast with the A2 overexpression, the overexpression of the A1 did not alter mitochondrial function under normoxia conditions

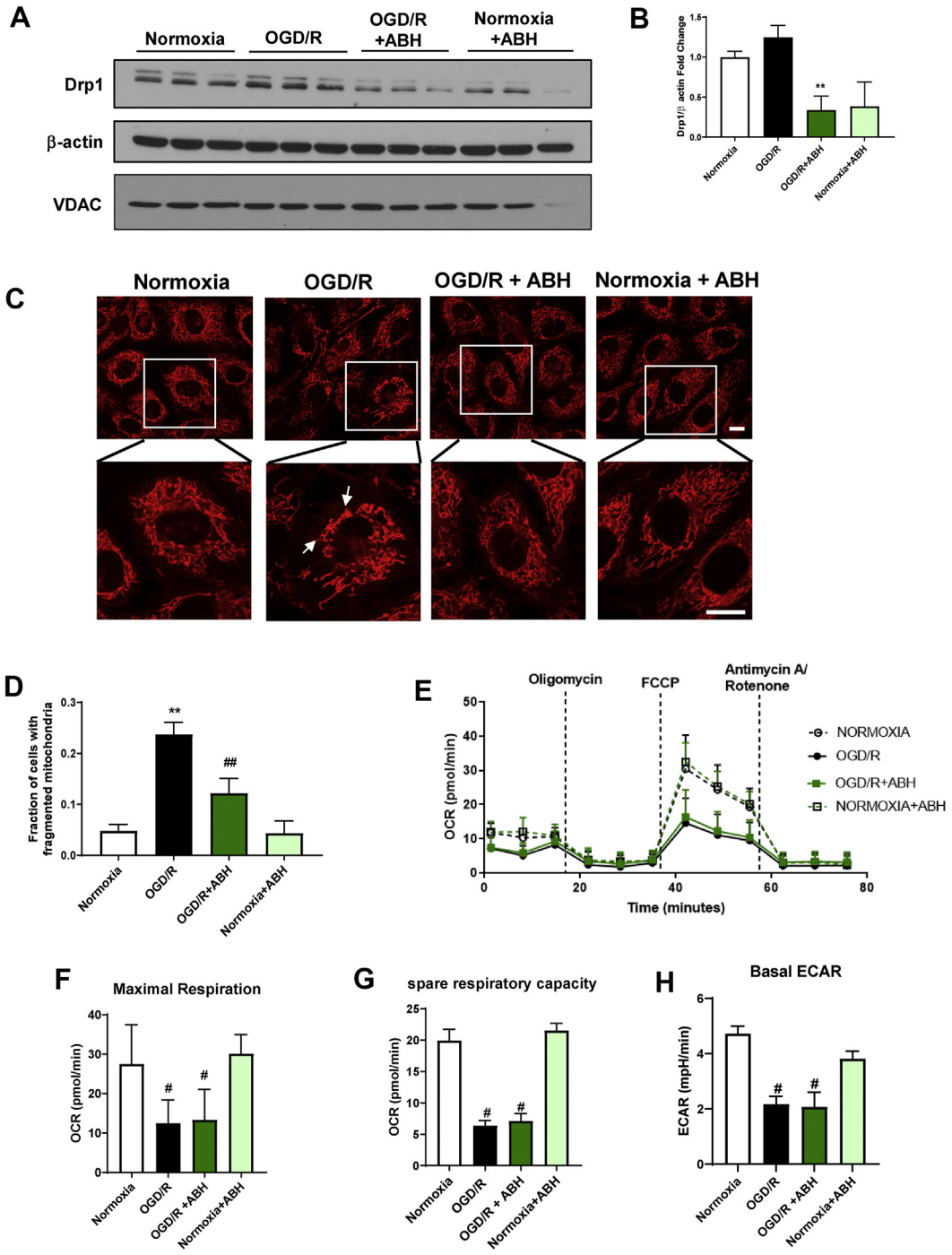

Figure 5: Arginase inhibition protects against OGD/R-induced mitochondrial fission but not impairment of mitochondrial respiration in BREC. A) Western blot analysis and quantification (B) showing ABH treatment significantly reduced Drp1 expression after OGD/R. $^{**}P < 0.01$ vs. normoxia. $n = 3$. C) Confocal images of mitochondria labeling using Rhodamine 123 with quantification (D) showing elongated and interconnected mitochondria under normoxic conditions versus punctate and fragmented mitochondria after OGD/R. ABH treatment reduced mitochondrial fragmentation. Insets show enlarged images of individual cells. $^{*}P < 0.05$ vs. normoxia. #$P < 0.05$ vs. OGD and normoxia. Scale bar $= 10$ μm, $n = 3$. E) Measurement of oxygen consumption rate (OCR, pmol/min) using Seahorse shows a decreased OCR with OGD/R. ABH did not affect OCR levels under normoxic or OGD/R conditions, $n = 9-44$. F) Maximal respiration showing a significant decrease after OGD/R compared to normoxic conditions. ABH did not protect against OGD/R-induced mitochondrial dysfunction. #$p < 0.001$ vs. normoxia. G) Spare respiratory capacity showing a significant decrease after OGD/R compared to normoxic conditions. ABH did not protect against OGD/R-induced mitochondrial dysfunction. #$p < 0.001$ vs. normoxia. H) Basal extracellular acidification rate (ECAR, pmol/min) is decreased after OGD/R. ABH did not protect against OGD/R-induced glycolysis impairment. #$p \leq 0.001$ vs. normoxia. Data are presented as mean ± SD.

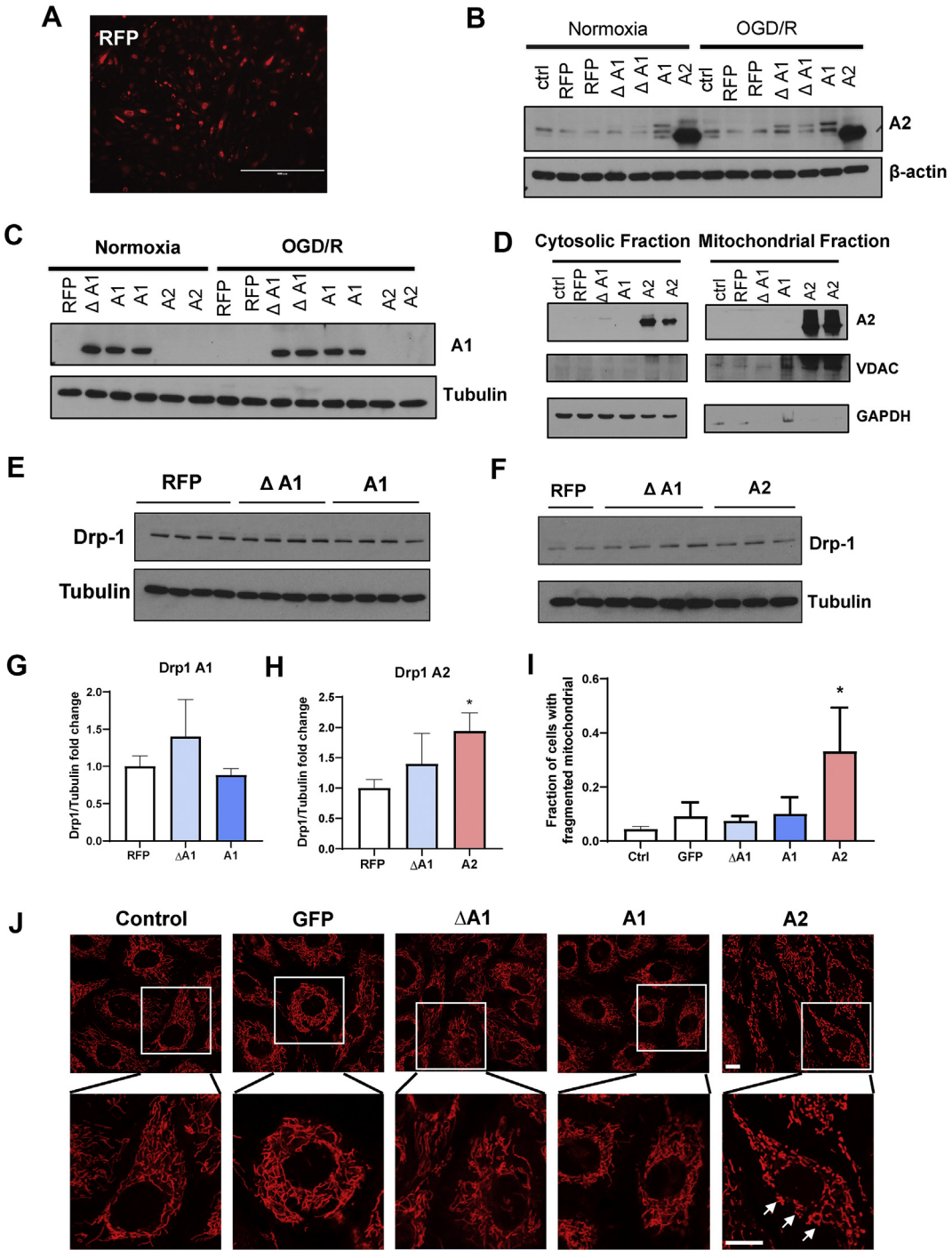

Figure 6: A2 overexpression induces mitochondrial fragmentation in BREC. A) Fluorescent microscopic image showing RFP expression in BRECs. Scale bar = 400 μm. B) and C) Western blot analyses showing the protein levels of A1 and A2 in BRECs transduced with 20 MOI of wild-type A1 (A1), wild-type A2 (A2), inactive mutant A1 (Δ A1), or red fluorescence protein (RFP) adenovirus vectors. n = 3. D) Western blot analyses showing the relative levels of A1 and A2 protein in cytosolic and mitochondrial fractions using the mitochondrial marker, VDAC, and the cytosolic marker, GAPDH. E) and F) Western blot analyses with quantification (G and H) showing increased expression of Drp1 in BRECs transduced with A2 compared to BRECs transduced with RFP, ΔA1, and A1. *$p < 0.05$ vs. all other groups. n = 3–8. Data are presented as mean ± SD. J) Confocal images of mitochondria labeled with Rhodamine 123 with quantification (I) in living BRECS showing the A2 overexpression-induced mitochondrial fragmentation as shown by punctate mitochondria compared to the interconnected mitochondrial network in other groups. Insets show enlarged images of individual cells. *$P < 0.05$ vs. other groups. Scale bar = 10 μm, n = 3.

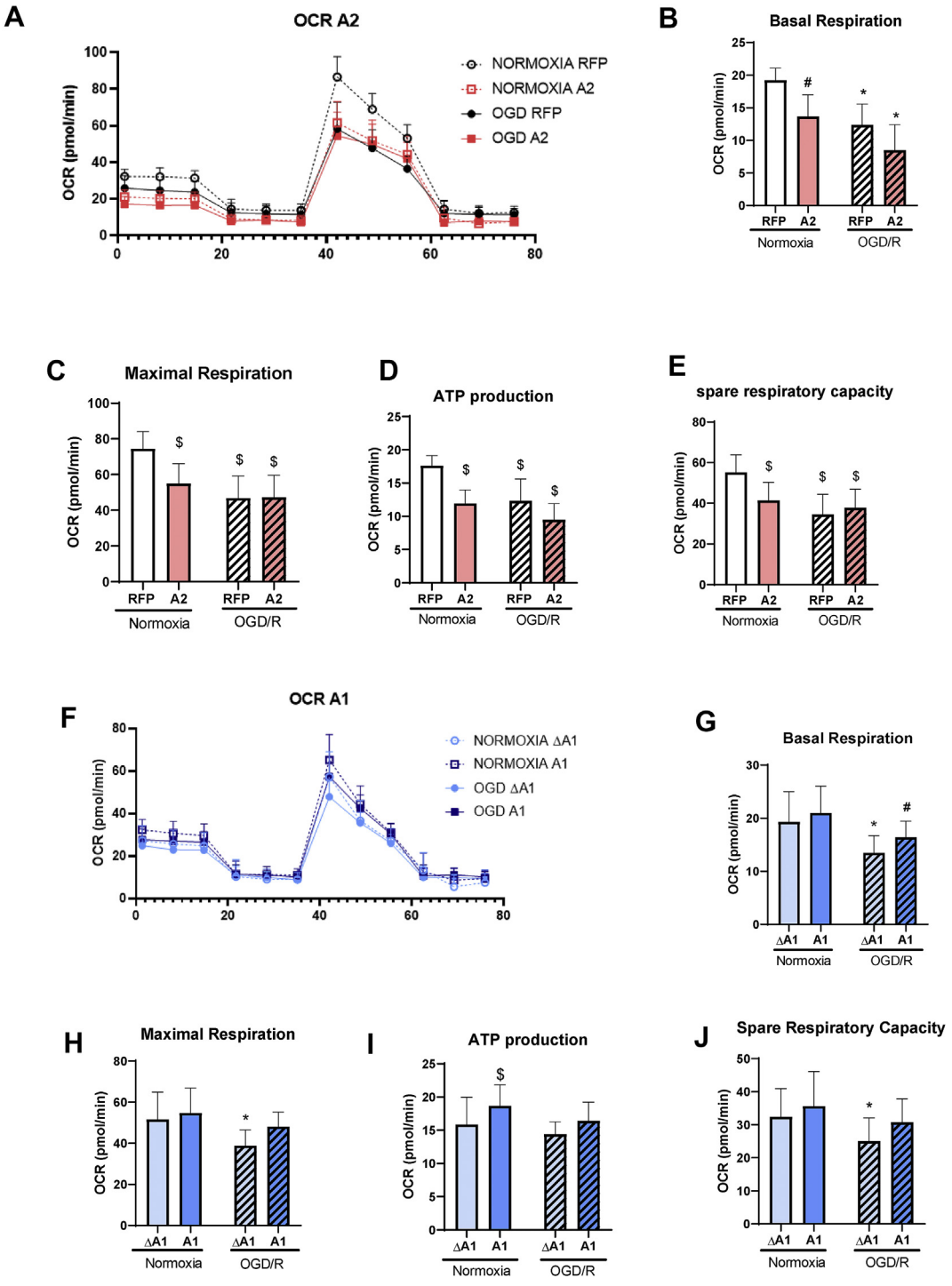

Figure 7: A2 overexpression impairs mitochondrial respiration in BREC while A1 overexpression limits OGD/R-induced dysfunction. A) Oxygen consumption rate (OCR) measured in BRECs using Seahorse showing decreased OCR with OGD/R. n = 10–24. B) Basal respiration, C) maximal respiration, D) ATP production, and E) Spare respiratory capacity showing a decreased OCR in the OGD/R RFP group compared to normoxia RFP. The overexpression of A2 showed a similar pattern of decreased OCR in both normoxia and OGD/R conditions. *P < 0.05 vs. normoxia A2 and Normoxia RFP. #P < 0.05 vs. normoxia RFP and OGD RFP. n = 10–24. $P < 0.05 vs. normoxia RFP. n = 10–24. F) OCR graph showing a decreased OCR with 5 h OGD/1 h R. n = 10–24. G) Basal respiration, H) maximal respiration, i) ATP production, and J) Spare respiratory capacity showing a decreased OCR in OGD/R ΔA1 group compared to normoxia groups. The overexpression of A1 protected against OGD/R-induced mitochondrial dysfunction*P < 0.05 vs. normoxia ΔA1 and normoxia A1. #P < 0.05 vs. normoxia A1. $P < 0.05 vs. normoxia ΔA1 and OGD ΔA1. n = 10–24. Data are presented as mean ± SD.

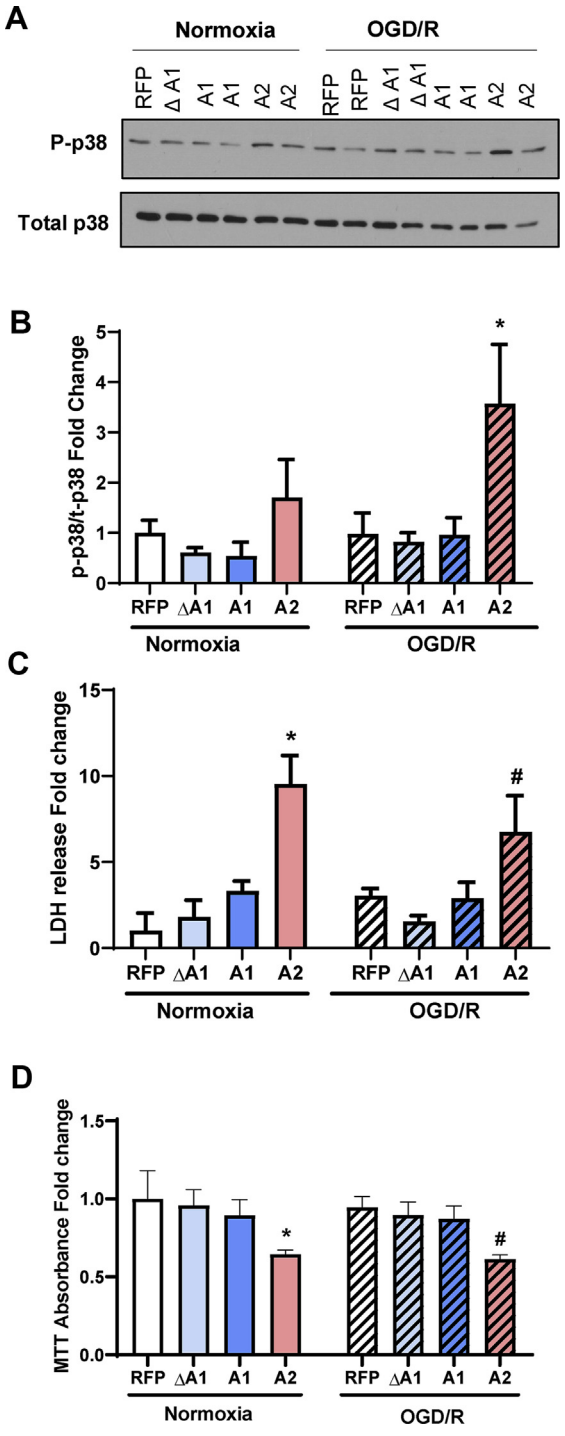

Figure 8: A2 overexpression increases cell stress and cell death in BREC. A) Western blot analysis with quantification (B) showing increased phosphorylation of the p38MAPK in BRECs transduced with A2 compared to cells transduced with Δ A1, A1, and RFP. *p $<$ 0.05 vs. all other groups. n $=$ 4–5 C) LDH release into the media collected from BRECs subjected to OGD/R is increased in cells transduced with A2 compared to other groups. *p $<$ 0.05vs. All groups except A2 OGD/R. #p $<$ 0.05 vs. all groups except A2 normoxia. n $=$ 3–4. d) MTT [3-(4,5-dimethylthiazol-2-yl)-2,5-diphenyltetrazolium bromide] absorbance in BRECs subjected to OGD/R showing decreased cell survival as indicated by decreased MTT absorbance in cells transduced with A2 compared to other groups. *p $<$ 0.05 vs. all groups except A2 OGD/R. #p $<$ 0.05vs. all groups except A2 normoxia. n $=$ 12–24. Data are presented as mean $\pm$ SD.

(Figure 7F–J). Moreover, the OGD/R-induced impairment of mitochondrial function was significantly blunted in the A1 group, indicating the significant preservation of mitochondrial function after OGD/R (Figure 7F–J). These data suggest distinct roles of the two arginase isoforms in the mitochondrial function of endothelial cells. Of note, the RFP and ΔA1 groups used as controls for the A2 and A1 overexpression experiments, respectively, were comparable under both normoxic and OGD/R conditions (Fig. S5)

2.5. A2 overexpression increases endothelial cell stress

We examined the effects on cell stress by a western blot analysis of P-p38 MAPK to investigate the differential roles of A1 vs. A2 overexpression in OGD/R-induced endothelial cell injury. The data showed that P-p38 MAPK was increased under normoxic conditions with the overexpression of A2 (Figure 8A&B) but not A1. We further evaluated the effect of A1 and A2 overexpression on cell death by measuring the release of lactate dehydrogenase (LDH) into the media. Under normoxic conditions, the LDH release after A2 overexpression was significantly elevated (~3-fold) compared with A1 overexpression (Fig. 8C). The OGD/R treatment did not further increase LDH release after the overexpression of either A1 or A2. We further confirmed the effect of A2 overexpression on cell survival by measuring the MTT absorbance. MTT formation was significantly decreased with A2 overexpression but not A1 overexpression under both normoxia and OGD/R conditions, indicating reduced cell survival (Fig. 8D).

3. DISCUSSION

In the present study, we explored the effect of A2-induced alterations in mitochondrial function in promoting ischemia/reperfusion-induced vascular injury. We found that the global deletion of A2 protects against the I/R-induced disruption of retinal structure and vascular permeability. Our analysis further showed that endothelial cell-specific A2 deletion protected against the I/R-induced neurodegeneration. We further showed that OGD/R insult induces an increase in BREC A2 expression, which is associated with mitochondrial dysfunction and fragmentation, along with the elevation of cell stress markers and increased cell death. The AAV-induced overexpression of A2 in BRECs resulted in a similar impairment of mitochondrial function and mitochondrial fragmentation, as well as increases in cell stress and cell death.

I/R insult is an established experimental model of retinal neurovascular degeneration [24]. Using the same mouse model, we have previously shown that I/R induces the thinning of the retinal layers along with neuronal loss in the GCL layer [3]. Here, we utilized fundus imaging and spectral domain optical coherence tomography (SD-OCT) to image the retina in living mice. These methods are widely used to assess retinal structural alterations in humans and animal models. A previous study used SD-OCT analysis in a mouse model of I/R to show progressive retinal thinning after I/R, especially in the inner plexiform and inner nuclear layers [25]. Histological studies from our lab have further confirmed the thinning of the entire retina and inner nuclear layer after I/R [3]. Our current OCT results show a disruption in the retinal layers and edema in the outer retina reduced with A2 deletion. This finding confirms our earlier histological finding that A2 induced retinal distortion after I/R insult [3]. In a mouse model of retinal ischemia induced by central artery occlusion, fundus examination showed edema and a whitening of the retina [26]. We observed a similar pathology with the fundus examination of WT mice, whereas A2KO retinas appeared normal after the I/R insult. These findings demonstrate the involvement of A2 in a similar pathology seen in patients with

retinal ischemic diseases. Potential mechanisms involve oxidative stress, glial activation, and inflammation, shown in various models of retinopathy [3,10,27].

I/R insult not only induces neuronal damage in the retina but also causes vascular injury [5]. Studies performed by Antonetti and colleagues have shown that I/R induces retinal vascular permeability as early as 4 h after the insult with a maximum leakage at 48 h in a vascular endothelial growth factor receptor-2 (VEGFR-2) dependent manner [28–30]. Here, we evaluated the retinal vascular permeability by measuring the extravasation of albumin and found that I/R induced significant leakage 48 h after the insult. The retinas of the A2KO mice showed significantly less vascular leakage compared to their WT littermates. We have previously shown that the global deletion of A2 reduced the formation of acellular capillaries after I/R [3]. The protective effect of A2 deletion in limiting acellular capillary formation and the blood-retinal barrier breakdown suggested that endothelial A2 is a critical player in mediating I/R-induced retinal neurovascular injury.

To assess the involvement of endothelial cell expression of A2 in retinal I/R injury, we performed studies using EC-specific A2 deletion. We found that the specific deletion of A2 in EC significantly protected against I/R-induced neurodegeneration. In contrast, myeloid-cell specific A2 deletion had no effect. The exact mechanisms regarding how endothelial A2 expression contributes to I/R injury are still unclear. However, given the mitochondrial localization of A2, we hypothesized that alterations in mitochondrial function are potentially involved. Using a mouse model, a recent study of chronic kidney disease showed that endothelial A2 causes renal fibrosis through altering mitochondrial function, decreasing NO levels, and increasing oxidative stress [31].

Oxygen-glucose deprivation/reperfusion has been widely used as an in vitro model to study the molecular mechanisms of I/R injury. Using endothelial cells subjected to OGD/R, we showed that A2 expression was induced by the injury and accompanied by an increase in cell stress and cell death markers. Hypoxia-induced increases in A2 expression have been previously reported in other ECs, including aortic and pulmonary EC [32,33]. Hypoxia has been shown to induce A2 mRNA and protein levels in pulmonary ECs through increases in hypoxia-inducible factor-2 (HIF-2) [34]. Interestingly, we found that treatment with the global arginase inhibitor, ABH, significantly protected against OGD/R-induced cell stress but did not prevent cell death. This effect may be due to ABH's ability to inhibit both A1 and A2 isoforms, which may have opposite influences on retinal I/R injury. We have previously shown that A2 deletion inhibits neurovascular injury after retinal I/R insult [3], whereas A1 deletion worsens I/R-induced neurovascular degeneration by exacerbating the macrophage inflammatory response [18]. Thus, the discrepancy in the ABH effects on cell stress vs. cell survival is potentially due to the differing roles of A1 and A2 in cell survival function. There is no specific inhibitor for either A1 or A2 to date.

We further explored the potential contribution of alterations in mitochondrial dynamics and function in the retinal OGD/R injury. Their involvement in I/R injury in different organs is well established [23,35–38]. Here, we have shown that OGD/R induced an increase in Drp1 expression that was blocked by arginase inhibition. Mitochondrial imaging showed an altered pattern of fragmented/punctate mitochondria in cells subjected to OGD/R compared with the elongated mitochondria seen in the normoxic condition. Cells subjected to OGD/R and treated with ABH showed improved mitochondrial morphology. Studies using the Seahorse XF analyzer showed further impaired mitochondrial function with OGD/R not rescued by the ABH treatment. Mitochondrial dynamics and function are profoundly tightly regulated processes. Any defect or imbalance in these processes is detrimental and can contribute to the pathology of different neurovascular degenerative diseases [39,40]. Indeed, mitochondria involved in retinal ganglion apoptotic cell death after I/R through the cyclophilin D-mediated mitochondrial opening of the permeability transition pore (MPTP) has been reported [41].

As noted earlier, there is no specific A2 inhibitor. We utilized different genetic manipulations to overexpress the two arginase isoforms and explore their distinct roles in OGD/R injury. We found that the overexpression of A2, but not A1, increased mitochondrial fission, as demonstrated by increased Drp1 expression and increased formation of punctate mitochondria. The exact mechanisms by which A2 induces the expression of Drp1 are not known. Future studies are needed to elucidate those mechanisms. One possible mechanism includes the interaction of the receptor and the protein 3 (RIP3)/Drp1 axis. A previous study has shown that RIP3 can activate Drp1 and induce its translocation in mitochondria, causing mitochondrial damage [42]. Previously, we have shown that A2 caused neuronal cell death by necroptosis through the induction of RIP3 expression [3]. Further studies are needed to assess whether A2 induces mitochondrial fragmentation by activating the RIP3/Drp1 axis.

Cell death is a hallmark of neurovascular degeneration in retinal I/R injury. Researchers, including us, have described I/R-induced neuronal and vascular cell death [3–5]. In the present study, we have shown that the overexpression of A2, but not A1, induces cell death and activates cell stress pathways. Further studies are needed to delineate the exact mechanisms of A2-induced cell death, though A2 may cause cell death by inducing oxidative stress. In a previous study, we demonstrated that A2 deletion reduces the formation of superoxide and nityrotyrosine in retinal I/R tissues [3]. Oxidative stress is known to be involved in the cell death mechanisms in neurodegenerative diseases [43]. It has been shown that A2 induces cell apoptosis/senescence through the activation of extracellular signal-regulated kinases (ERKs) and the sequential activation of 40S ribosomal protein S6 kinase 1 (S6K1)-c-Jun N-terminal kinases (JNKs) [44].

Surprisingly, despite A2 existing in the mitochondria, no studies have ever looked at the role of A2 in mitochondrial dynamics or function in endothelial cells to our knowledge. The physiological functions of A2 are poorly understood, though it has been speculated to be crucial in polyamine and proline synthesis [45]. The polyamine pathway can be dysregulated under pathological conditions, leading to deleterious outcomes [46–48]. In addition to producing polyamines, studies in a model of atherosclerosis have shown that the elevation of A2 promotes EC dysfunction by a mechanism involving increases in mitochondrial calcium and P32 levels [49]. Though further work is required to define the role of A2 in normal mitochondrial function, our study is the first to show a potential involvement of A2 upregulation in promoting mitochondrial fission and dysfunction in endothelial cells. Interestingly, a very recent study found that A2 is involved in IL-10 mediated mitochondrial fusion in macrophages, suggesting the different effects of A2 on the mitochondrial dynamics in different cell types [50]. Here we showed that A2 overexpression induces mitochondrial dysfunction in normoxic conditions, as demonstrated by the reduction of basal respiration, maximal respiration, ATP production, and spare respiratory capacity. A previous study by Ming et al. has shown that the overexpression of A2 in smooth muscle cells increases the formation of mitochondrial reactive oxygen species and decreases mitochondrial membrane potential independently of its L-arginine ureahydrolase activity [44]. A later study showed the same effect of A2 expression on mitochondria, resulting in p38 MAPK activation and increased chemokine production [51]. Other potential mechanisms of I/R-induced mitochondrial dysfunction potentially include mitophagy or A2-

mediated increases in polyamine metabolism. Alterations in VEGF and VEGFR2 signaling are also possibly involved in the A2-induced vascular injury in retinal I/R injury. Further studies are needed to explore other mechanisms for A2-induced mitochondrial dysfunction and neurovascular injury after I/R.

In conclusion, this study is the first to show that endothelial A2 is crucial in mediating the retinal I/R injury. The deletion of A2 in endothelial cells protected against I/R-induced neuronal degeneration. In vitro studies confirmed that the overexpression of A2 in retinal vascular endothelial cells induces cell stress and cell death, increases mitochondrial fragmentation, and promotes mitochondrial dysfunction.

4. MATERIALS AND METHODS

4.1. Animals and ischemia/reperfusion (I/R) insult

All procedures with animals were performed following the ARVO Statement for the Use of Animals in Ophthalmic and Vision Research and were approved by the institutional animal care and use committee (Animal Welfare Assurance no. A3307—01). All surgeries were performed under anesthesia, and all efforts were made to minimize suffering. WT and global A2KO mice on C57BL6 background were generated in our animal colony as described previously [3,10,15]. The floxed A2 transgenic mice were obtained from Dr. Dmitri Firsov's lab, then rederived in Jackson laboratories in a C57BL-6 background [52]. The cell-specific A2 KO was generated as previously described [18]. Floxed A2 mice were crossed with Cre-expressing transgenic mice under the control of either a VE-Cadherin promoter ($Cdh5^{Cre}$) or lysozyme 2 promoter ($LysM^{Cre}$) to generate either endothelial-specific A2KO (E— A2KO) or myeloid-specific A2KO (M— A2KO) mice, respectively.

I/R injury in the right eye was done as previously described [3]. Mice (10—12 weeks old) were anesthetized with 73 mg/kg Ketamine Hydrochloride and 7.3 mg/kg Xylazine Hydrochloride, ip. 1% tropicamide (Akorn, Lake Forest, IL) was used to dilate the pupil, and topical anesthesia (0.5% proparacaine hydrochloride [Akorn]) was applied to the cornea. The anterior chamber of the right eye was cannulated with a 30-gauge needle to infuse sterile saline. The saline reservoir was elevated to raise the intraocular pressure to 110 mm Hg and held for 40 min. To confirm ischemia, we studied the whitening of the anterior segment of the globe and blanching of episcleral veins [53]. The left eye was used as a sham control. We sacrificed the mice at different time points, depending on outcome measures and existing literature.

4.2. Retinal histology

The histology of retinal sections was evaluated as previously described [3]. Eyeballs were collected and snap-frozen in an Optimal Cutting Temperature (O.C.T) compound. Cross-sections with optic nerve attachment were prepared (10 μm), followed by H&E staining for morphological observation.

4.3. Retinal neuronal quantification

Eyeballs were collected 7 days after I/R injury and fixed overnight in 4% PFA. Retinas were dissected and immunolabelled with the neuronal marker, NeuN, as previously described [3]. Flatmount images in the mid-periphery of the ganglion cell layer (four from each retina) were taken using a Zeiss LSM 780 Inverted Confocal microscopy (Carl Zeiss AG, Oberkochen, Germany) with a 20x lens, and NeuN positive cells were quantified as previously described [3].

4.4. Cell culture and oxygen-glucose deprivation/reperfusion model

Bovine retinal endothelial cells (BRECs) from passages 4—8 were used for the cell culture studies. BRECs were isolated by our group as previously described [54]. Cells were grown in an M199 media containing 10% fetal bovine serum (FBS), 1% Penicillin/Streptomycin (Gimini, West Sacramento, CA), and 10% cell systems complete media until 70—80% confluency was reached. For OGD/R experiments, cells were shifted to serum starvation M199 media containing 0.2% FBS and 0.1% bovine serum albumin (BSA) overnight. The next day, media was changed to a glucose-free DMEM media (Thermo Fisher, Waltham, MA), supplemented with 1% penicillin/streptomycin, and the cells were kept in $<1\%$ oxygen in a hypoxia chamber for different periods of time, as mentioned in the results. After the specified OGD time, media were changed to normal complete media, and cells were kept in normoxic conditions for the specified time to achieve reperfusion. Normoxia control cells were maintained in complete media under normoxic conditions. Cells were then processed for western blotting or mitochondria labeling. Cells were treated with or without the arginase inhibitor 2(S)-amino-6-boronohexanoic Acid (ABH) (100 μM).

4.5. Arginase overexpression

Cells were transduced with adenoviral vectors as previously described with modifications [55]. Briefly, cells (P4—P7) were grown to a confluence of 70%—80% and then transduced with adenoviral vectors containing A1, A2, ΔA1, RFP, or GFP for 6 h at a 20 multiplicity of infection (MOI). In the ΔA1 construct, the aspartic acid 128 was mutated to glycine (D128G) [55,56]. This mutation disrupts the binding pocket for manganese, which is a crucial activity of either isoform [57]. The ΔA1 is present at the expected molecular weight of the wild-type arginase but has a complete loss of activity [56]. The MOI was chosen according to previously published studies and preliminary experiments (Fig. S6) [55]. The composition of the media used for transduction is as follows: low arginine M199 (Gibco) supplemented with 50 μM L-arginine, 0.2% FBS, and 0.1% BSA. After 6 h, the media was changed to normal complete growth media, and the cells were incubated to recover for 24 h. The following day, the transduction efficiency was evaluated by checking the fluorescence of the control proteins (RFP or GFP) using a fluorescence microscope. After reaching 100% confluence, the cells were split into Seahorse cell culture plates, 6-well plates, or glass-bottom dishes, depending on the outcome measures and then subjected to OGD/R insult or normoxia, as described above.

4.6. Measurement of lactate dehydrogenase (LDH) release into the media

The LDH release into the media was measured using the Cytotoxicity Detection Kit^{PLUS} (Sigma, St. Louis, MO). Cells were subjected to OGD/R or normoxia, as explained above, then media were collected after the end of the reperfusion. The media were centrifuged at 250 *g* for 10 min and then processed to measure the LDH release, following the manufacturer's instructions.

4.7. MTT ((3-(4,5-dimethylthiazol-2-yl)-2,5-diphenyltetrazolium bromide) assay

Cells were transduced as explained above and plated in 96-well plates for the MTT assay. The cells were subjected to OGD/R or normoxia, as explained earlier. Then, the cells were processed according to the manufacturer's instructions to evaluate cell survival using the MTT probe (Thermo Fisher, Waltham, MA).

4.8. Mitochondrial isolation

Cells were plated in 100 mm Petri dishes. Then, arginase isoforms were overexpressed as described above. Cells were then processed to isolate the mitochondrial fraction using the mitochondrial isolation kit for cultured mammalian cells (Thermo Fisher, Waltham, MA) following the manufacturer's instructions.

4.9. Mitochondrial labeling

Cells were cultured in glass-bottom dishes, and OGD/R or the normoxia control was performed as explained above. VectaCellTM Rhodamine 123 (Vector Laboratories, Burlingame, CA) was used to label mitochondria in live cells as previously reported [18]. Briefly, cells were washed three times with modified phosphate buffered saline containing 1 mM CaCl2 and 0.5 mM MgCl2 (PBS +; Thermo Fisher, Waltham, MA). The cells were incubated with the Rhodamine 123 staining solution at 37 °C for 15 min and rinsed three times with PBS+. We used adenoviral control vectors expressing GFP instead of RFP for the mitochondrial labeling of transduced BRECs, as Rhodamine 123 fluoresces red. Live cell images were taken using a Zeiss LSM 780 Inverted Confocal microscopy (Carl Zeiss AG, Oberkochen, Germany) with a 63x lens. Four random images per dish were taken, and the numbers of cells with fragmented mitochondria were counted and divided by the total number of cells per image to get the fraction of cells with fragmented mitochondria [50]. Averages of the four images from each data set were calculated to represent an individual data point in the final graph.

4.10. Seahorse XF96 mito stress test

A Mito stress test (Agilent, Catalogue # 103015-100, Santa Clara, CA) and Seahorse XF96 (Agilent, Santa Clara, CA) were used to evaluate mitochondrial dysfunction. Briefly, Seahorse cell culture plates were used to grow the cells. BRECs (p4-6) were seeded at a cell density of 4 K/well in the Seahorse cell culture plate coated with 0.2% gelatin in all the wells except A1, A12, H1, and H12 wells, which were used as background wells. Cells were kept growing in normal complete media for 24 h. The following day, cells were switched to serum-free media overnight and then subjected to OGD/R or control conditions. For transduced BRECs, we overexpressed the cells and then kept the cells growing to confluence. After this procedure, cells were plated in the Seahorse cell culture plates at a cell density of 4 K/well and subjected to OGD/R or control conditions, as described above. The day before the assay, the Seahorse media were prepared according to the manufacturer's instructions and supplemented with 2.5 mM glutamine (Gimini, West Sacramento, CA) and 5.5 mM glucose (Sigma, St. Louis, MO). Then, we ran the Mito stress test according to the manufacturer's instructions. The concentrations of the injection compounds used were Oligomycin (2 μM), FCCP (2 μM), and Rotenone/antimycin A (0.5 μM). The data were collected and analyzed using the Wave software (Agilent, Santa Clara, CA).

4.11. Fundus imaging and spectral domain optical coherence tomography (SD-OCT)

Fundus imaging and SD-OCT were done as previously described [58,59]. Briefly, 2% isoflurane was used to anesthetize the mice, and their pupils were dilated using 1% tropicamide eye drops. Mice were placed on the imaging platform of the Phoenix Micron III retinal imaging microscope, supplemented with an OCT imaging device (Phoenix Research Laboratories, Pleasanton, CA). Genteal gel was applied during imaging to keep the eye moist. Four images were taken for each mouse eye.

4.12. Western blot analysis

Western blotting was performed as previously described [3]. Briefly, retinal or endothelial cell lysates were extracted using a RIPA buffer (Millipore, Billerica, MA) containing 1x protease and phosphatase inhibitors (Complete Mini and phosSTOP, respectively; Roche Applied Science, Indianapolis, IN). Proteins were separated on SDS-PAGE and transferred to a nitrocellulose membrane (Millipore, Billerica, MA), and then blocked in 5% milk (Bio-Rad, Hercules, CA). For the albumin extravasation experiment, the mice were transcardially perfused with PBS as previously described to clear out the blood, and then retinas were collected and processed as described above [18].

The primary antibodies were Arginase-2 (Santa Cruz Biotechnology Cat. # Sc-20151, Dallas, Texas, 1:500), arginase 1 (Santa Cruz Biotechnology, Dallas, TX, USA; Cat. # Sc-20150; 1:500), phospho p38 (Cell Signaling Technology Cat. # 4511, Danvers, MA, 1:500), total p38 (Cell Signaling Technology Cat. # 9212, Danvers, MA, 1:500), Drp1 (Santa Cruz Biotechnology Cat. # Sc-271583, Dallas, Texas, 1:500), PARP (Cell Signaling Technology Cat. # 9542, Danvers, MA, 1:500), VDAC (Cell Signaling Technology, Cat. # 4661, Danvers, MA, 1:500), GAPDH (Meridian Life Science Cat. #H86504M, Memphis, TN, 1:5000), albumin (Bethyl Laboratories, Montgomery, TX, 1:10000), tubulin (Sigma—Aldrich Cat. # T-9026, St. Louis, MO, 1:5000), and β-actin (Sigma—Aldrich Cat. # A1978, St. Louis, MO, 1:5000). Primary antibodies were diluted in either 5% milk or 5% bovine serum albumin (BSA). Membranes were incubated with the primary antibodies overnight. The next day, membranes were washed in TBST (Tris-buffered saline with 0.5% Tween-20), and horseradish peroxidase-conjugated secondary antibodies (GE Healthcare, Piscataway, NJ) were added (1:5000 for tubulin and actin and 1:1000 for others). An enhanced chemiluminescence system (GE Healthcare Bio-Science Corp., Piscataway, NJ) was used to detect immunoreactive proteins. Data were quantified by densitometry using image J and normalized to the loading control.

4.13. Statistical analysis

Data are presented as mean ± SD. GraphPad Prism 8 (GraphPad Softwar Inc., La Jolla, CA, USA) was used for statistical analysis. A two-way ANOVA or one-way ANOVA followed by a Tukey test or Holm-Sidak for multiple comparisons (or a two-tailed student's t-test in the case of single comparisons) was used. $P \leq 0.05$ was considered statistically significant. For cell culture studies, experiments were repeated at least twice in different independent batches of cells. Only one set of experiments is presented in the cell culture figures.

ACKNOWLEDGMENTS

This work was supported in part by grants from The National Institute of Health: [R01- EY011766 (RBC, RWC), R01-EY030500 (RBC), R21EY032265 (RBC), K99 award: 1K99EY029373-01A1 (AYF)], the Department of Veterans Affairs, Veterans Health Administration (RBC), Office of Research and Development, Biomedical Laboratory Research and Development: BX001233 (RBC), American Heart Association 15PRE25560007 (ES), and NIH Core grant P30EY031631. R. B. Caldwell is a VA Research Career Scientist VA IK6BX005228. The contents do not represent the views of the Department of Veterans Affairs or the United States Government. The funders had no role in the study design, data collection and analysis, decision to publish, or preparation of the manuscript.

CONFLICT OF INTEREST

None declared.

APPENDIX A. SUPPLEMENTARY DATA

Supplementary data to this article can be found online at https://doi.org/10.1016/j.molmet.2021.101273.

REFERENCES

[1] Osborne, N.N., Casson, R.J., Wood, J.P., Chidlow, G., Graham, M., Melena, J., 2004. Retinal ischemia: mechanisms of damage and potential therapeutic strategies. Progress in Retinal and Eye Research 23(1):91—147.

[2] Minhas, G., Sharma, J., Khan, N., 2016. Cellular stress response and immune signaling in retinal ischemia-reperfusion injury. Frontiers in Immunology 7:444.

[3] Shosha, E., Xu, Z., Yokota, H., Saul, A., Rojas, M., Caldwell, R.W., et al., 2016. Arginase 2 promotes neurovascular degeneration during ischemia/reperfusion injury. Cell Death & Disease 7(11):e2483.

[4] Yokota, H., Narayanan, S.P., Zhang, W., Liu, H., Rojas, M., Xu, Z., et al., 2011. Neuroprotection from retinal ischemia/reperfusion injury by nox2 nadph oxidase deletion. Investigative Ophthalmology & Visual Science 52(11):8123—8131.

[5] Zheng, L., Gong, B., Hatala, D.A., Kern, T.S., 2007. Retinal ischemia and reperfusion causes capillary degeneration: similarities to diabetes. Investigative Ophthalmology & Visual Science 48(1):361—367.

[6] Caldwell, R.B., Toque, H.A., Narayanan, S.P., Caldwell, R.W., 2015. Arginase: an old enzyme with new tricks. Trends in Pharmacological Sciences 36(6):395—405.

[7] Ash, D.E., Cox, J.D., Christianson, D.W., 2000. Arginase: a binuclear manganese metalloenzyme. Metal Ions in Biological Systems 37:407—428.

[8] Morris Jr., S.M., 2002. Regulation of enzymes of the urea cycle and arginine metabolism. Annual Review of Nutrition 22:87—105.

[9] Patel, C., Rojas, M., Narayanan, S.P., Zhang, W., Xu, Z., Lemtalsi, T., et al., 2013. Arginase as a mediator of diabetic retinopathy. Frontiers in Immunology 4:173.

[10] Narayanan, S.P., Suwanpradid, J., Saul, A., Xu, Z., Still, A., Caldwell, R.W., et al., 2011. Arginase 2 deletion reduces neuro-glial injury and improves retinal function in a model of retinopathy of prematurity. PloS One 6(7):e22460.

[11] Narayanan, S.P., Xu, Z., Putluri, N., Sreekumar, A., Lemtalsi, T., Caldwell, R.W., et al., 2014. Arginase 2 deficiency reduces hyperoxia-mediated retinal neurodegeneration through the regulation of polyamine metabolism. Cell Death & Disease 5:e1075.

[12] Raup-Konsavage, W.M., Gao, T., Cooper, T.K., Morris Jr., S.M., Reeves, W.B., Awad, A.S., 2017. Arginase-2 mediates renal ischemia-reperfusion injury. American Journal of Physiology - Renal Physiology 313(2):F522—F534.

[13] Tratsiakovich, Y., Kiss, A., Gonon, A.T., Yang, J., Sjoquist, P.O., Pernow, J., 2017. Inhibition of rho kinase protects from ischaemia-reperfusion injury via regulation of arginase activity and nitric oxide synthase in type 1 diabetes. Diabetes and Vascular Disease Research 14(3):236—245.

[14] Erbas, H., Aydogdu, N., Kaymak, K., 2004. Effects of n-acetylcysteine on arginase, ornithine and nitric oxide in renal ischemia-reperfusion injury. Pharmacological Research 50(5):523—527.

[15] Suwanpradid, J., Rojas, M., Behzadian, M.A., Caldwell, R.W., Caldwell, R.B., 2014. Arginase 2 deficiency prevents oxidative stress and limits hyperoxia-induced retinal vascular degeneration. PloS One 9(11):e110604.

[16] Bitner, B.R., Brink, D.C., Mathew, L.C., Pautler, R.G., Robertson, C.S., 2010. Impact of arginase ii on cbf in experimental cortical impact injury in mice using mri. Journal of Cerebral Blood Flow and Metabolism 30(6):1105—1109.

[17] Hansmannel, F., Sillaire, A., Kamboh, M.I., Lendon, C., Pasquier, F., Hannequin, D., et al., 2010. Is the urea cycle involved in alzheimer's disease? Journal Alzheimer's Disease 21(3):1013—1021.

[18] Fouda, A.Y., Xu, Z., Shosha, E., Lemtalsi, T., Chen, J., Toque, H.A., et al., 2018. Arginase 1 promotes retinal neurovascular protection from ischemia through suppression of macrophage inflammatory responses. Cell Death & Disease 9(10):1001.

[19] Schmid, H., Renner, M., Dick, H.B., Joachim, S.C., 2014. Loss of inner retinal neurons after retinal ischemia in rats. Investigative Ophthalmology & Visual Science 55(4):2777—2787.

[20] Yuan, Y., Zheng, Y., Zhang, X., Chen, Y., Wu, X., Wu, J., et al., 2017. Bnip3l/nix-mediated mitophagy protects against ischemic brain injury independent of park2. Autophagy, 1—13.

[21] Wang, H., Zheng, S., Liu, M., Jia, C., Wang, S., Wang, X., et al., 2016. The effect of propofol on mitochondrial fission during oxygen-glucose deprivation and reperfusion injury in rat hippocampal neurons. PloS One 11(10):e0165052.

[22] Zhao, Y.X., Cui, M., Chen, S.F., Dong, Q., Liu, X.Y., 2014. Amelioration of ischemic mitochondrial injury and bax-dependent outer membrane permeabilization by mdivi-1. CNS Neuroscience and Therapeutics 20(6):528—538.

[23] Chen, J.L., Duan, W.J., Luo, S., Li, S., Ma, X.H., Hou, B.N., et al., 2017. Ferulic acid attenuates brain microvascular endothelial cells damage caused by oxygen-glucose deprivation via punctate-mitochondria-dependent mitophagy. Brain Research 1666:17—26.

[24] Hartsock, M.J., Cho, H., Wu, L., Chen, W.J., Gong, J., Duh, E.J., 2016. A mouse model of retinal ischemia-reperfusion injury through elevation of intraocular pressure. Journal of Visualized Experiments(113).

[25] Kim, B.J., Silverman, S.M., Liu, Y., Wordinger, R.J., Pang, I.H., Clark, A.F., 2016. In vitro and in vivo neuroprotective effects of cjun n-terminal kinase inhibitors on retinal ganglion cells. Molecular Neurodegeneration 11:30.

[26] Goldenberg-Cohen, N., Dadon, S., Avraham, B.C., Kramer, M., Hasanreisoglu, M., Eldar, I., et al., 2008. Molecular and histological changes following central retinal artery occlusion in a mouse model. Experimental Eye Research 87(4):327—333.

[27] Xu, Z., Fouda, A.Y., Lemtalsi, T., Shosha, E., Rojas, M., Liu, F., et al., 2018. Retinal neuroprotection from optic nerve trauma by deletion of arginase 2. Frontiers in Neuroscience 12:970.

[28] Abcouwer, S.F., Lin, C.M., Wolpert, E.B., Shanmugam, S., Schaefer, E.W., Freeman, W.M., et al., 2010. Effects of ischemic preconditioning and bevacizumab on apoptosis and vascular permeability following retinal ischemia-reperfusion injury. Investigative Ophthalmology & Visual Science 51(11):5920—5933.

[29] Abcouwer, S.F., Lin, C.M., Shanmugam, S., Muthusamy, A., Barber, A.J., Antonetti, D.A., 2013. Minocycline prevents retinal inflammation and vascular permeability following ischemia-reperfusion injury. Journal of Neuroinflammation 10:149.

[30] Muthusamy, A., Lin, C.M., Shanmugam, S., Lindner, H.M., Abcouwer, S.F., Antonetti, D.A., 2014. Ischemia-reperfusion injury induces occludin phosphorylation/ubiquitination and retinal vascular permeability in a vegfr-2-dependent manner. Journal of Cerebral Blood Flow and Metabolism 34(3):522—531.

[31] Wetzel, M.D., Stanley, K., Wang, W.W., Maity, S., Madesh, M., Reeves, W.B., et al., 2020. Selective inhibition of arginase-2 in endothelial cells but not proximal tubules reduces renal fibrosis. JCI Insight 5(19).

[32] Wang, L., Bhatta, A., Toque, H.A., Rojas, M., Yao, L., Xu, Z., et al., 2015. Arginase inhibition enhances angiogenesis in endothelial cells exposed to hypoxia. Microvascular Research 98:1—8.

[33] Pandey, D., Nomura, Y., Rossberg, M.C., Hori, D., Bhatta, A., Keceli, G., et al., 2018. Hypoxia triggers senp1 (sentrin-specific protease 1) modulation of klf15 (kruppel-like factor 15) and transcriptional regulation of arg2 (arginase 2) in pulmonary endothelium. Arteriosclerosis, Thrombosis, and Vascular Biology 38(4):913—926.

[34] Krotova, K., Patel, J.M., Block, E.R., Zharikov, S., 2010. Hypoxic upregulation of arginase ii in human lung endothelial cells. American Journal of Physiology - Cell Physiology 299(6):C1541—C1548.
[35] Gong, Z., Pan, J., Shen, Q., Li, M., Peng, Y., 2018. Mitochondrial dysfunction induces nlrp3 inflammasome activation during cerebral ischemia/reperfusion injury. Journal of Neuroinflammation 15(1):242.
[36] Imai, T., Mishiro, K., Takagi, T., Isono, A., Nagasawa, H., Tsuruma, K., et al., 2017. Protective effect of bendavia (ss-31) against oxygen/glucose-deprivation stress-induced mitochondrial damage in human brain microvascular endothelial cells. Current Neurovascular Research 14(1):53—59.
[37] Liao, L.X., Zhao, M.B., Dong, X., Jiang, Y., Zeng, K.W., Tu, P.F., 2016. Tdb protects vascular endothelial cells against oxygen-glucose deprivation/reperfusion-induced injury by targeting mir-34a to increase bcl-2 expression. Scientific Reports 6:37959.
[38] Tang, C., Han, H., Liu, Z., Liu, Y., Yin, L., Cai, J., et al., 2019. Activation of bnip3-mediated mitophagy protects against renal ischemia-reperfusion injury. Cell Death & Disease 10(9):677.
[39] Westermann, B., 2010. Mitochondrial fusion and fission in cell life and death. Nature Reviews Molecular Cell Biology 11(12):872—884.
[40] Anzell, A.R., Maizy, R., Przyklenk, K., Sanderson, T.H., 2018. Mitochondrial quality control and disease: insights into ischemia-reperfusion injury. Molecular Neurobiology 55(3):2547—2564.
[41] Kim, S.Y., Shim, M.S., Kim, K.Y., Weinreb, R.N., Wheeler, L.A., Ju, W.K., 2014. Inhibition of cyclophilin d by cyclosporin a promotes retinal ganglion cell survival by preventing mitochondrial alteration in ischemic injury. Cell Death & Disease 5(3):e1105.
[42] Wang, X., Jiang, W., Yan, Y., Gong, T., Han, J., Tian, Z., et al., 2014. Rna viruses promote activation of the nlrp3 inflammasome through a rip1-rip3-drp1 signaling pathway. Nature Immunology 15(12):1126—1133.
[43] Radi, E., Formichi, P., Battisti, C., Federico, A., 2014. Apoptosis and oxidative stress in neurodegenerative diseases. Journal Alzheimer's Disease 42(Suppl 3):S125—S152.
[44] Xiong, Y., Yu, Y., Montani, J.P., Yang, Z., Ming, X.F., 2013. Arginase-ii induces vascular smooth muscle cell senescence and apoptosis through p66shc and p53 independently of its l-arginine ureahydrolase activity: implications for atherosclerotic plaque vulnerability. Journal American Heart Association 2(4):e000096.
[45] Wu, G., Morris Jr., S.M., 1998. Arginine metabolism: nitric oxide and beyond. Biochemical Journal 336(Pt 1):1—17 (Pt 1).
[46] Narayanan, S.P., Xu, Z., Putluri, N., Sreekumar, A., Lemtalsi, T., Caldwell, R.W., et al., 2014. Arginase 2 deficiency reduces hyperoxia-mediated retinal neurodegeneration through the regulation of polyamine metabolism. Cell Death & Disease 5(2):e1075.
[47] Patel, C., Xu, Z., Shosha, E., Xing, J., Lucas, R., Caldwell, R.W., et al., 2016. Treatment with polyamine oxidase inhibitor reduces microglial activation and limits vascular injury in ischemic retinopathy. Biochimica et Biophysica Acta 1862(9):1628—1639.
[48] Fouda, A.Y., Eldahshan, W., Narayanan, S.P., Caldwell, R.W., Caldwell, R.B., 2020. Arginase pathway in acute retina and brain injury: therapeutic opportunities and unexplored avenues. Frontiers in Pharmacology 11:277.
[49] Koo, B.H., Hwang, H.M., Yi, B.G., Lim, H.K., Jeon, B.H., Hoe, K.L., et al., 2018. Arginase ii contributes to the ca(2+)/camkii/enos axis by regulating ca(2+) concentration between the cytosol and mitochondria in a p32-dependent manner. Journal American Heart Association 7(18):e009579.
[50] Dowling, J.K., Afzal, R., Gearing, L.J., Cervantes-Silva, M.P., Annett, S., Davis, G.M., et al., 2021. Mitochondrial arginase-2 is essential for il-10 metabolic reprogramming of inflammatory macrophages. Nature Communications 12(1):1460.
[51] Koo, B.H., Yi, B.G., Jeong, M.S., Kwon, S.H., Hoe, K.L., Kwon, Y.G., et al., 2018. Arginase ii inhibition prevents interleukin-8 production through regulation of p38 mapk phosphorylation activated by loss of mitochondrial membrane potential in nldl-stimulated haosmcs. Experimental & Molecular Medicine 50(2):e438.
[52] Ansermet, C., Centeno, G., Lagarrigue, S., Nikolaeva, S., Yoshihara, H.A., Pradervand, S., et al., 2020. Renal tubular arginase-2 participates in the formation of the corticomedullary urea gradient and attenuates kidney damage in ischemia-reperfusion injury in mice. Acta Physiologica 229(3):e13457.
[53] Da, T., Verkman, A.S., 2004. Aquaporin-4 gene disruption in mice protects against impaired retinal function and cell death after ischemia. Investigative Ophthalmology & Visual Science 45(12):4477—4483.
[54] Behzadian, M.A., Wang, X.L., Jiang, B., Caldwell, R.B., 1995. Angiostatic role of astrocytes: suppression of vascular endothelial cell growth by tgf-beta and other inhibitory factor(s). Glia 15(4):480—490.
[55] Shosha, E., Xu, Z., Narayanan, S.P., Lemtalsi, T., Fouda, A.Y., Rojas, M., et al., 2018. Mechanisms of diabetes-induced endothelial cell senescence: role of arginase 1. International Journal of Molecular Sciences 19(4).
[56] Elms, S., Chen, F., Wang, Y., Qian, J., Askari, B., Yu, Y., et al., 2013. Insights into the arginine paradox: evidence against the importance of subcellular location of arginase and enos. American Journal of Physiology - Heart and Circulatory Physiology 305(5):H651—H666.
[57] Vockley, J.G., Tabor, D.E., Kern, R.M., Goodman, B.K., Wissmann, P.B., Kang, D.S., et al., 1994. Identification of mutations (d128g, h141l) in the liver arginase gene of patients with hyperargininemia. Human Mutation 4(2):150—154.
[58] Ibrahim, A.S., Tawfik, A.M., Hussein, K.A., Elshafey, S., Markand, S., Rizk, N., et al., 2015. Pigment epithelium-derived factor inhibits retinal microvascular dysfunction induced by 12/15-lipoxygenase-derived eicosanoids. Biochimica et Biophysica Acta 1851(3):290—298.
[59] Ibrahim, A.S., Mander, S., Hussein, K.A., Elsherbiny, N.M., Smith, S.B., Al-Shabrawey, M., et al., 2016. Hyperhomocysteinemia disrupts retinal pigment epithelial structure and function with features of age-related macular degeneration. Oncotarget 7(8):8532—8545.

